



Original scientific paper

UDC: 621.548-047.44(497.16)
<https://doi.org/10.2298/IJGI2501033Z>


Received: July 26, 2024

Reviewed: November 29, 2024

Accepted: January 30, 2025



ENHANCING WIND ENERGY PRODUCTION ESTIMATION OVER MONTENEGRO USING MODELED AND OBSERVED WIND SPEEDS AND SYNOPTIC WEATHER PATTERNS

Aleksandar Zečević¹, Dragana Vujović^{2*} 

¹Institute of Hydrometeorology and Seismology, Podgorica, Montenegro; e-mail: zecevic050@gmail.com

²University of Belgrade, Faculty of Physics, Department of Meteorology, Belgrade, Serbia; e-mail: dvujovic@ff.bg.ac.rs

Abstract: This study analyses the wind conditions over complex terrain and evaluates wind resources based on synoptic weather patterns. The wind direction showed a pronounced north-south bidirectionality. The cut-out speed occurs infrequently and is mainly limited to the north-east and south-south-east winds. The observed wind speeds at location Krnovo (Nikšić) verified the wind forecast of the Weather Research and Forecasting Non-Hydrostatic Mesoscale Model (WRF NMM). The model slightly underestimated the lower average hourly wind speeds; the errors were greatest during the winter season. The best forecast was for one day ahead. The correlation coefficients between the observed and predicted winds at 90 m height for one, two, and three days ahead were 0.85, 0.83, and 0.82, respectively. The synoptic situations were analyzed to identify the underlying weather patterns that favour maximum and minimum energy production lasting most of the day. Maximum energy production was associated with a deep trough over western Europe extending in a northwest-southeast direction and a pronounced meridional meandering jet stream. A ridge or anticyclone over the Balkan Peninsula, a more or less zonal jet stream and strong warm air advection over Montenegro characterized the atmosphere during the periods of minimum energy production. Together with reliable wind forecasts, these results can improve the use of renewable energies in the future and make them more efficient.

Keywords: wind power; wind rose; synoptic situation; WRF NMM; forecast verification; Krnovo (Nikšić)

1. Introduction

According to projections of the US Energy Information Administration (EIA, 2021), the share of renewable energies in electricity generation in the USA will double by 2050, from 21% today to 42%. It is assumed that renewable energy sources will account for 47% of total consumption by 2050, with the greatest growth in solar and wind energy sources (EIA, 2021). This means that the use of energy sources closely related to atmospheric conditions is likely to increase in the future and meteorological research will play a key role in the field of environmental sustainability. A high-quality prediction of meteorological variables will consequently provide a high-quality projection for electricity generation at different locations. On 4 February 2025,

*Corresponding author, e-mail: dvujovic@ff.bg.ac.rs

Montenegro was between 20 top countries in Europe by the wind power share in the country's electricity mix with 24.7% (Association for Wind Energy in Europe, 2025). In 2023, wind power in Montenegro contributed 7.7% to the country's electricity production (Ministarstvo energetike i rudarstva, 2024).

Wind power is proportional to the third power of wind speed, which means that accurately predicting the power output of wind farms could significantly reduce the cost of operating the electricity grid (Đurišić & Mikulović, 2012). Therefore, wind speed is a very important parameter for verifying wind power (Lazić et al., 2010). Burlando et al. (2009) suggested that Montenegro (orig. Crna Gora), together with neighboring countries, has a high potential for the development of significant wind energy production. Numerous studies have analyzed the geospatial potential for using wind energy in Serbia (Đurišić & Mikulović, 2012; Potić et al., 2021). The need for an accurate wind power forecast, which depends on the quality of the numerical weather prediction model (NWP), is understandable from the point of view of ensuring a stable energy supply. Two main sources of error in forecasts are the imperfection of the prediction models and the uncertainties in the observations. Despite the enormous progress that has been made in this field, reliable predictions are limited to a forecasting period of less than ten days (Krishnamurthy, 2019). In Lazić et al. (2010), the regional NWP model Eta was applied and the wind forecasting for wind turbines in Sweden was validated. In a later study, the authors proposed to improve the wind prediction of the NWP Eta model with the newly proposed Model Output Statistics method (Lazić et al., 2014). The Weather Research and Forecasting (WRF) model has recently been used for wind farm planning (Bilal et al., 2016; Cuevas-Figueroa et al., 2022; Souza et al., 2023; Tan et al., 2021).

The complex topography significantly influences the wind field in the lower layer of the atmosphere and causes strong turbulent flow due to frictional force. This adjusts the air pressure field relative to the topography (Wood & Mason, 1993). As a result, the wind patterns differ between the mountain regions and the prevailing wind directions. A large part of Montenegro is covered by high and extensive mountain massifs, characterized by mountains higher than 2,000 m along the Dinaric Alps, cut by river gorges and deep valleys (Frank et al., 2016).

There is a close relationship between atmospheric circulation and wind power production, which means that the most frequently recurring large-scale atmospheric patterns could be used as a tool to understand atmospheric variability. Studies on synoptic situations that favor the optimal production of wind energy at a certain location are rare. Steiner et al. (2017) investigated wind energy production in Germany and looked at the errors in forecasting wind power for the day and their link to the underlying weather situations. The authors concluded that the greatest errors in wind power forecasts occur when cyclones and lows move across the North Sea, Baltic Sea, or Germany. In addition, Köhler et al. (2017) investigated the effects of forecasts of low cloud cover on the quality of the photovoltaic power prediction and concluded that fog and a stratus cloud cause one-third of the days with the highest forecast errors.

This study has several objectives. The intention was to determine the characteristics of the wind field based on the special wind measurements in the Krnovo Mountain in Montenegro. By comparing the wind speed predictions with the observed wind field, it could be estimated how reliably the regional Weather Research and Forecasting Non-Hydrostatic Mesoscale Model (WRF NMM) can predict the wind over complex terrain. Through the analysis of wind data, this study seeks to identify atmospheric circulation patterns that promote optimal (MxEP) and minimal (MnEP) energy production at our site. Achieving these goals would greatly

enhance the ability to manage wind energy production effectively. By evaluating the anticipated synoptic conditions, it is possible to ascertain the potential maximum energy output at a specific location. This analysis will provide valuable insights for management, enabling more effective optimization of energy generation strategies. This study is the first of its kind in Montenegro and the entire region.

2. Data and methods

2.1. Study area: Geographical and climate characteristics

The Krnovo wind farm is located on the plateau of the same name in the central part of Montenegro ($\lambda = 19.11^\circ\text{E}$, $\varphi = 42.89^\circ\text{N}$), about 20 km north-east of Nikšić ($\lambda = 18.94^\circ\text{E}$, $\varphi = 42.77^\circ\text{N}$). The farm comprises 26 wind turbines and is the first wind farm in Montenegro and one of the largest wind parks in the region (Figure 1). Krnovo is a plateau with an average altitude of 1,500 m a.s.l., the highest point of which is called Krnovska glavica (1,608 m a.s.l.). It is rectangular with a length of 12 km from north-west to south-east and 10 km from north-east to south-west (Zorić, 1976). The area is characterized by a mountainous climate with short summers and long, cold, and snowy winters with frequent frosts and low temperatures (Burić et al., 2012). The Krnovo area has an average wind speed ranging from 5.5 to 6.5 m/s. Additionally, the area is equipped with road and electricity network infrastructure. These factors contributed to the decision to select this location for the wind farm that was installed in 2017 (Italian Ministry for the Environment, Land and Sea, 2007). In 2023, wind power in Montenegro contributed 7.7% to the country's electricity production (Ministarstvo energetike i rudarstva, 2024).



Figure 1. Location of Krnovo wind farm (19.11°E , 42.89°N) in the northern part of Montenegro, northeast of Nikšić (18.94°E , 42.77°N). The inner rectangle indicates the locations of wind turbines in Krnovo.

2.2. Wind analysis

The standard height for measuring wind speed in meteorology is 10 m. However, for the analyses here, 10-minute averaged values of wind speed and direction were used measured at the hub height of a wind turbine at 90 m for two years from 2019 to 2020. Acuoenergy Firm, the company that manages the Krnovo wind farm (Masdar, n.d.), has provided us with the observed wind data. Promoting innovation in solar, wind, energy storage, waste-to-energy, and geothermal energy, the company has developed projects in more than 40 countries across six continents with a combined capacity of more than 31.5 GW. A total of 104,303 measurements were taken into account, corresponding to 99.09% of all possible data. A Weibull distribution provides a good approximation to a histogram of wind speed and is often used when analyzing wind energy resources (Carta et al., 2009; Đurišić & Mikulović, 2012; Romanić et al., 2018). The Weibull distribution (Weibull, 1951) visualizes the probability of a particular mean wind speed occurring at a particular location at a specific time:

$$f(u) = \left(\frac{k}{A}\right) \left(\frac{u}{A}\right)^{k-1} e^{-\left(\frac{u}{A}\right)^k} \quad (1)$$

where $f(u)$ is the frequency of occurrence of a certain wind speed u (m/s), A (m/s) and k are the scale and shape parameters, respectively. The values of k are between 1 and 3, with small values representing very variable winds, while large values correspond more to constant wind values. The value A is proportional to the mean wind speed. The values for A and k were calculated by adjusting the actual distribution of wind speed values (Burlando et al., 2009; Romanic et al., 2018).

2.3. Power curve, cut-in, and cut-out speed

The power curve shows the relationship between the output of the wind turbine and the average wind speed at hub height. It is usually determined based on field measurements (Tong, 2010). The turbine starts to produce usable energy when the wind speed reaches a certain threshold, the so-called cut-in wind speed (Landberg, 2016). If the wind speed is very high, the turbine switches off to avoid excessive loads (cut-out wind speed). The cut-in and cut-out wind speeds of many commercial turbines are 3 and 25 m/s, respectively, which is also the case here. The maximum (MxEP) energy production at the site is defined with the wind speeds in the interval (14, 25 m/s). The minimum or no energy production (MnEP) is for the wind speeds $v \leq 3$ m/s.

2.4. Verification of the WRF NMM

Analytically unsolvable non-linear differential equations are an obstacle to calculating the future state of the atmosphere. However, this problem can be overcome using numerical methods. Since the atmosphere is a deterministic chaos that depends on numerous variables that are variable in time and space and influence each other directly and indirectly, even a small initial error can cause large future errors. Against this background, NWP models and parametric schemes describing the processes in the subgrids at the existing model resolution, as a set of equations and various numerical and interpolation techniques, cannot provide perfectly accurate solutions. The WRF NMM developed at National Centers

for Environmental Prediction (NCEP), version 3.9.1, was used in this analysis as the atmospheric model for wind forecast (Janjic, 2003; Janjic et al., 2001). A vertical coordinate in the model is a hybrid sigma coordinate that follows the terrain. This approach allows a more accurate simulation of the airflow over complex terrain. The model solves compressible non-hydrostatic dynamical equations. The global model of the European Centre for Medium-Range Weather Forecasts (ECMWF) with a global resolution of $dx = dy = 0.125$ degrees was used for the initialization of the WRF model. Subsequently, the model was run with a resolution of 3 km and the results were used as boundary conditions for the WRF NMM with a horizontal resolution of 1 km. For the planetary boundary layer, the parameterization according to Janjić (1994) was used. The model is operational at the Institute for Hydrometeorology and Seismology in Montenegro. The model has been utilized for a variety of forecasting and verification purposes (Fonseca et al., 2020; Valappil et al., 2020).

There is the significant bias in wind speed found in WRF simulations for areas with complex topography (Jiménez & Dudhia, 2013; Wyszogradzki et al., 2013). The wind forecasts over forecast periods of 24, 48, and 72 hours were verified using the observed winds at a height of 90 m at the specified location Krnovo for the first time as far as we know. Verification of forecasted wind speeds by WRF NMM at a height of 2 m was previously done (Zečević et al., 2023). In the current study, the model started at 00 UTC with a horizontal resolution of 1 km. The vertical resolution from the surface to a height of 50 hPa is sixty sigma levels. The model verification was performed only for the year 2020, as the Institute's memory resources were limited and only GRIB files for one year could be stored. Nevertheless, it is a respectable number of predicted–observed pairs of hourly wind speed for 363 days. For comparison, Lazić et al. (2010) made verification of the Eta model for three summers, 333 days in total. Lee et al. (2022) evaluated wind speed and power prediction for only 2 and 7 days.

There is a variety of verification techniques, all of which concern the relationship between a prediction or a set of predictions and the corresponding observation or observations to which they refer (Wilks, 2006). Currently, three common scalar measures of prediction accuracy are used for continuous variables: the mean absolute error (MA), the mean error (ME), and the mean squared error (MSE) or the root mean square error (RMSE). The calculation of the mean difference provides an estimate of the model. It shows how often and to what extent the model underestimates or overestimates a forecast of a certain variable.

3. Results and discussion

3.1. Analysis of the measured wind field

The measured data on wind speed and direction is statistically analyzed. This includes frequency of occurrence, probability density function, wind rose and annual statistics. Some basic statistics on the observed 10-minute mean wind speeds can be found in Figure 2D and Appendix A, Table A1. The wind speed production potential at the wind farm was the highest in winter when the demand for electrical energy was the greatest. The most important findings are as follows.

Figures 2A and 2B show a wind rose with 16 directions and the frequency distribution of wind speeds, which show a Weibull-like distribution at the wind farm site. As it can be seen from the diagram in Figure 2A, the concentric circles represent the frequency of 16 wind directions. The prevailing winds are northerly (N, NNW, NNE) and southerly (SSE, SE, S) with

an overall frequency of 65%. The most common wind direction among the 16 is north (N), accounting for 13% of the total. This can also be observed from the concentric circle representing this frequency. South-southeast winds were observed almost in 13% of the time. Winds from the west and east (west-southwest, west-northwest, east-southeast, and east-northeast) were rarely observed, totaling less than 13% of the time. The different colors of the wind rose mark different intervals of wind speeds. The radius of the concentric circles with a step size of 2.0% represents the frequency of the wind speed. The most frequent wind speeds were in the interval from 4 to 12 m/s. The prevailing wind directions at this location are indeed the strongest and the northerly winds were somewhat stronger than the southerly ones. The interval of the highest wind speeds above 16 m/s was most pronounced in the south-easterly (0.56%) and south-south-easterly directions (0.59%). This distribution of the most frequent winds was very favorable from the point of view of wind resources.

To determine the days with the most favorable wind conditions, the wind data measured at a height of 90 m was used for two years, 2019 and 2020. However, the use of data from only two years is a limitation of the study: the more data analyzed, the more representative the conclusions. These data suggest the prevailing winds come from the northern and the southern quadrant. Krnovo is located on a mountain ridge and such an air flow has been typical for Nikšić for years. Indeed, Burić et al. (2012) suggested that significant winds in Montenegro are always associated with certain characteristic weather situations: the approach and passage of the cyclone from the Gulf of Genoa and the presence of an anticyclone northeast of Montenegro, as well as a combination of their mutual positions. This leads to the fact that the prevailing winds in Montenegro come from northern and southern directions, which is also concluded on the basis of two years of data. Accordingly, it is expected that this short period data will be sufficient to carry out a representative analysis.

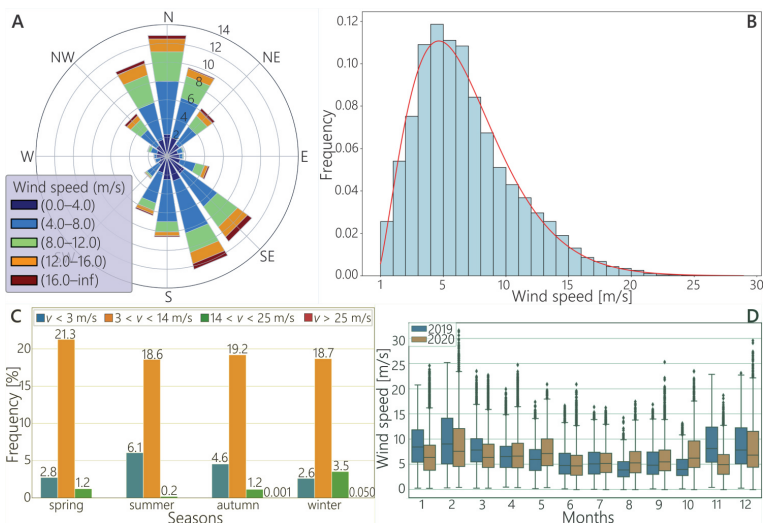


Figure 2. Wind rose (A), the relative frequency (B), seasonal (C), and monthly (D) distribution of wind speeds at the Krnovo wind farm, for 2019 and 2020.

The most frequently recorded wind speed was 5 m/s (Figure 2B). The data show that weak wind speeds between 0 and 3 m/s (when there is no energy production) occurred almost 16% of the time. This means that for more than 84% of the year, wind speeds were higher than 3 m/s, so the wind turbines were in operation for more than 7,380 hours per year (strong winds, higher than 25 m/s, were rare with occurrence of 0.05%, so the turbines were not frequently out of operation). Wind speeds suitable for MxEP (between 14 and 25 m/s) occur less frequently, in 6.14% of the time. The wind rose with highlighted significant wind speed intervals is given in Appendix A, Figure A2. Figure 2C shows the power output in the relationship of wind speeds by seasons. The season in which wind speeds associated with MxEP occurred most frequently was winter. These wind speeds were not only the most frequent but also the highest. Conversely, the events responsible for MnEP were the most frequent in summer and autumn. The winds exceeding 25 m/s occur with a total frequency of 0.051% and are observed only in autumn and winter.

Another insightful way to analyze the relationship between wind speeds and wind directions is to plot one against the other, as shown in Figure 3. Each point in the figure represents the pair of speed and direction at a particular date and time. The figure clearly shows that the cut-out wind speed was mainly limited to the specific wind direction at 50° and around 150°, corresponding to winds from the north-east and south-south-east. However, there was only a limited number of these events, indicating that they were short-lived and isolated extreme weather events. As there was a predominant direction, these events were caused by similar weather conditions, be it an isolated instability in summer or a snowstorm in winter blizzards. The diagram shows that blizzards in winter were responsible for these extreme wind speeds (blue dots denote winter events).

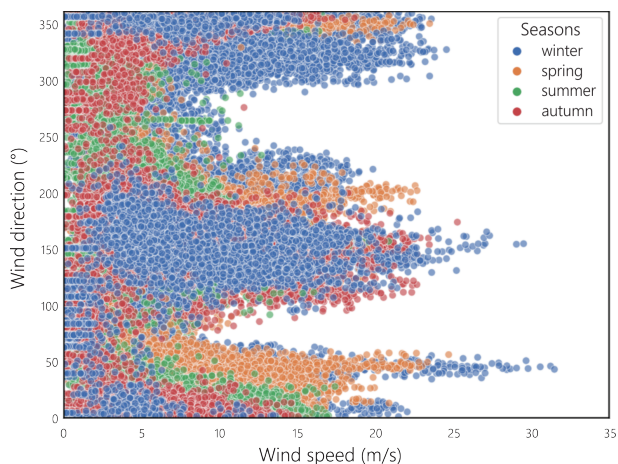


Figure 3. Speed (m/s) versus direction (°) of wind data for the specified location for four seasons.

In winter, late autumn and early spring, the average daily wind speeds were at their highest, decreasing slightly and steadily toward summer, when the lowest mean daily wind speeds were measured in June, July, and August. To determine the synoptic situation associated with the peaks in energy production, the weather on the day corresponding to the months and days when the MxEP (maximum energy production) lasted the longest was

Table 1. Dates and frequency of MnEP and MxEP

Date	MnEP ($v \leq 3$ m/s)	Date	MxEP ($14 \text{ m/s} \leq v < 25$ m/s)
12/12/2020	120	02/23/2019	134
06/26/2020	119	12/21/2019	134
12/21/2020	110	12/28/2020	130
08/13/2019	107	03/12/2019	127
06/16/2020	106	02/02/2019	123
07/21/2019	104	11/03/2019	120
08/18/2019	103	02/12/2019	116
09/16/2019	103	02/12/2019	115
01/15/2020	102	02/13/2019	110
08/29/2019	102	01/06/2020	110
10/23/2019	101	02/06/2020	110
06/21/2019	100	04/05/2020	105
09/02/2019	99	01/05/2020	101
08/28/2019	98	11/05/2019	99
07/31/2020	97	02/15/2019	98

analyzed. The frequency of MxEP events was the highest in winter months in both years. In July and August, there were only isolated MxEP events, which can be attributed to short-term summer instabilities. Two peaks were recorded where wind speeds of a selected strength were blowing for most of the day: 134 10-minute intervals, or 22.3 hours to be exact (a single day has 144 10-minute measurements). In 2020, the wind speeds in the interval of interest had their longest duration on December 28. The synoptic situation for this day will be described in more detail later. All the synoptic situations in which MxEP and MnEP lasted longer than 60% of the length of the entire day were analyzed.

Table 1 shows the first 15 such dates. The columns MnEP and MxEP represent the number of 10-minute intervals with wind speeds $v \leq 3$ m/s and $14 \text{ m/s} \leq v < 25$ m/s, respectively. The values are sorted in descending order. Of the 15 dates on which the MxEP was generated, 73% occurred in the winter season (December, January, February), while 13% occurred in spring or autumn. Not a single date was recorded in the summer season. As for the MnEP, 60% of the days were recorded in the summer season, while about 20% were recorded in the autumn and winter seasons. Not a single MnEP event was recorded in spring.

3.2. Analysis of synoptic situations for MxEP and MnEP

The reanalysis is a weather analysis that is not performed in real-time. The background field (i.e. a forecast from the previous analysis period) is generated by the NWP model and remains constant throughout the reanalysis period (American Meteorological Society, 2018). A reanalysis produces complete, globally gridded data that is as homogeneous as possible in time and provides a retrospective record of the global analysis of the atmospheric fields. All data were quality-controlled and assimilated using a data assimilation system that remained unchanged during the reanalysis period. Reanalysis is considered the best weather analysis.

The identification of days with optimal wind speeds for maximum energy production was based on the data of the observed wind speeds. These favorable days are then associated with corresponding synoptic conditions, which can usually be predicted more accurately than hourly wind speed values for a specific location. To achieve this, reanalysis data were used for 30 days listed in Table 1 to identify similarities in synoptic conditions based on two important and predictable meteorological parameters: geopotential at 500 mb and temperature at 850 hPa. The winds, air temperatures, and geopotential heights are from reanalyses by the NCEP, part of the National Oceanic and Atmospheric Administration. Characteristic situations for dates with MxEP and MnEP are described below.

3.2.1. MxEP

It has been decided to describe the analysis of the synoptic conditions on February 23, 2019, as wind speeds in the optimal range for MxEP were measured for 22.3 hours as on this day. Two troughs were recognized in the upper level height field of 500 hPa (Figure 4A). The first had a weaker intensity and crossed the Balkan Peninsula in the early hours of the morning. The strong low-pressure system with axes over Iceland, the south of Great Britain, the east of France, and the Gulf of Genoa, moved over Montenegro for the rest of the day. Stormy weather and colder air at the surface are usually the result of strong troughs caused by atmospheric fronts in the shallow layers of the atmosphere. On this particular day, there was a relatively warm air mass in the temperature field at 850 hPa over central, southeastern, and part of eastern Europe. However, a synoptic analysis of the surface map of Europe shows that precisely in those parts of the continent there was a well-defined anticyclone with cold air, which means that there was a temperature inversion that is characteristic of the winter months. This had the effect that over the ridge of the Dinarides mountain massif, which includes the mountainous part of Montenegro, cold air from the north was transferred to the Adriatic Sea and caused a strong north and northeast wind. At the site of Krnovo (1,500 m a.s.l.) there were favorable conditions for MxEP due to the strong northerly wind. Above that height, the wind changed direction to the southwest. The position and strength of the jet stream influence weather patterns at the Earth's surface. The jet stream refers to strong high-altitude winds that are concentrated in a narrow stream in the atmosphere. On the particular day, the jet stream was at 300 hPa and had a pronounced north-south direction over Central Europe and the Apennine Peninsula (Figure 4B). This type of synoptic situation was characteristic of all but one date (28.12.2020) of the MxEP. Therefore, conclusion is that the presence of a deep trough over Western Europe and the Bay of Genoa, together with a meandering jet stream, has created favorable weather conditions for the MxEP in the Krnovo wind farm. In all the cases of MxEP, the jet stream had a meandering character with a pronounced meridional component. The meridional component in Figure 4B is strongly noticeable from the Apennine Peninsula via Germany to the North Sea. The deep trough over Western Europe and the Gulf of Genoa and the meandering jet stream were responsible for the weather conditions that led to MxEP in the wind farm.

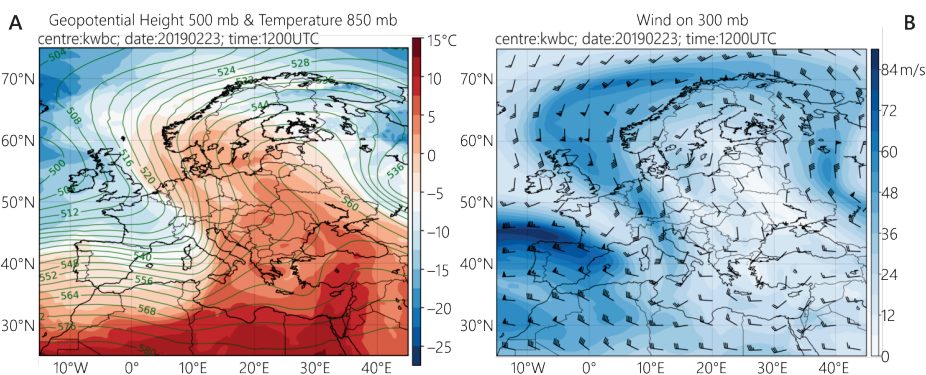


Figure 4. Geopotential at isobar surface of 500 hPa in gpdm and air temperature at 850 hPa in °C (A); wind at the height of 300 hPa in m/s (B) for 23.2.2019 in 12 UTC. Wind barbs indicate the wind direction and wind speed.

The second date from the list in Table 1 that was analyzed was December 28, 2020 (Figure 5). On this day, the wind speed remained in the optimal range for 130 intervals of 10 minutes each. Further analysis of the synoptic map showed the presence of a deep cyclone over the North Sea, with a closed isohypse of 488 gpdm in the centre. The cyclone affected the Mediterranean region in its periphery circulation, causing an advection of warm air from North Africa over the Balkans and creating a pronounced temperature gradient over Montenegro, although not an extreme one. The pressure gradient is most pronounced over the Western Mediterranean and Iberian Peninsula. However, the condensed isohypses over Montenegro also show a strong pressure gradient, which leads to strong winds in the region. This is supported by observed wind speeds ranging from 14 to 25 m/s (50–90 km/h) during 130 ten-minute intervals, totaling over 21 hours of data collected in one day. The jet stream had a pronounced zonal component over North Africa and the Mediterranean to the eastern Mediterranean. In this region, the jet stream changed direction and acquired a meridional component, which south-west winds over Montenegro confirms. Therefore, the jet stream had a meandering character with strong winds reaching up to 40 m/s directly over the Balkan Peninsula. This was a unique situation in the series of all the selected synoptic situations for MxEP, as the cyclone was located over the UK. It was a deep cyclone that exerted a strong peripheral influence on the region in question with the help of a meandering jet stream. This resulted in the best weather conditions for power generation, regardless of distance. During the recording of the MxEP, it was observed that on all other days, a cyclone was present over the Apennine Peninsula or a deep trough area extending northwest-southeast. The position of this cyclone allowed the formation of strong air pressure and temperature gradients, which led to strong winds from the south-west at 300 hPa. In all the cases of MxEP, the jet stream had a meandering character with a pronounced meridional component. The situation on February 23, 2019 is similar to the current situation regarding the trough of low pressure over the Ligurian and Tyrrhenian Sea. This suggests that the deep trough over Western Europe and the Gulf of Genoa and the meandering jet stream were responsible for the weather conditions that led to the MxEP at the Krnovo wind farm.

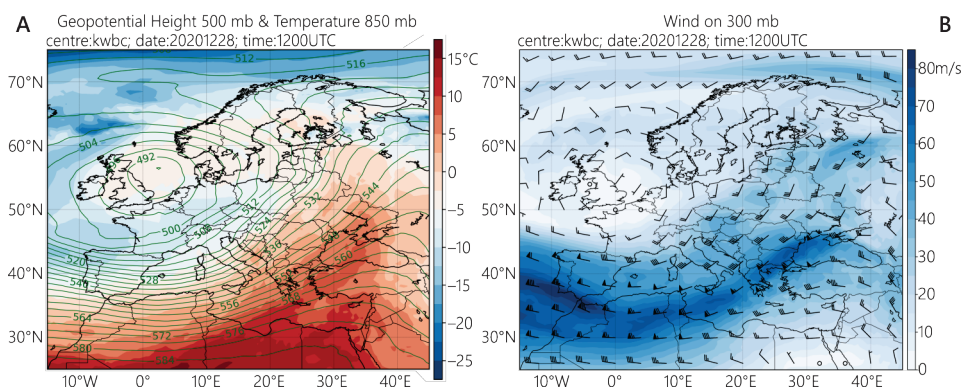


Figure 5. The same as Figure 4, but for 28.12.2020 in 12 UTC.

3.2.2. MnEP

In both years studied, the conditions with prolonged periods of low wind speeds, which made it impossible for the wind turbines to generate enough energy (i.e. when wind speeds were below 3 m/s), occurred most frequently during the summer season, which can be seen from Table 1 and in Appendix A, Table A1, that shows the lowest mean wind speeds for three summer months. During the summer months, a ridge with its axis over Africa or anticyclones with closed isohypses over the Ionian Sea or the Greek mainland were observed. In winter, the area of Montenegro was under the influence of a ridge or saddle aloft, together with a very pronounced warm air advection at the 850 hPa surface. The lower atmosphere was cold due to the increased radiation. The warm advection created a lid of warm air above, resulting in stable stratification with weak or no winds. The fifteen dates with the most favorable conditions for MnEP (the absence of the wind) were caused by an anticyclone or a ridge and the lack of a jet stream or an interrupted jet stream on the 300 hPa surface. In 80% of all cases were synoptic situations in which the jet stream was either far to the north of Montenegro or intermittent and disorganized. High-pressure situations in the saddle between two cyclones were characteristic of the remaining 20% of cases. Figure 6 illustrates a typical weather situation on June 26, 2020, when a strong ridge was located over the Balkan Peninsula. During this period, 119 10-minute intervals with wind speeds of less than or equal to 3 m/s were recorded. The center of the cyclone was located over the Pyrenees. The warm sector of the cyclone is above the Balearic Islands and in the direction of Corsica, Sardinia, and the South Adriatic. According to the wind measurements at the Krnovo site, the cyclone did not have such a large impact that it could influence the weather in Montenegro significantly. In addition, the axis of the jet stream was located north of Montenegro. The goal of the research was to recognize similarities between the synoptic situations in which energy production either reached its maximum or its minimum. For this reason, the wind at 300 hPa was analyzed and not the wind at 850 hPa, as this is nearly the altitude of the Krnovo site and the analysis would be strongly affected by the influence of the surface/drag.

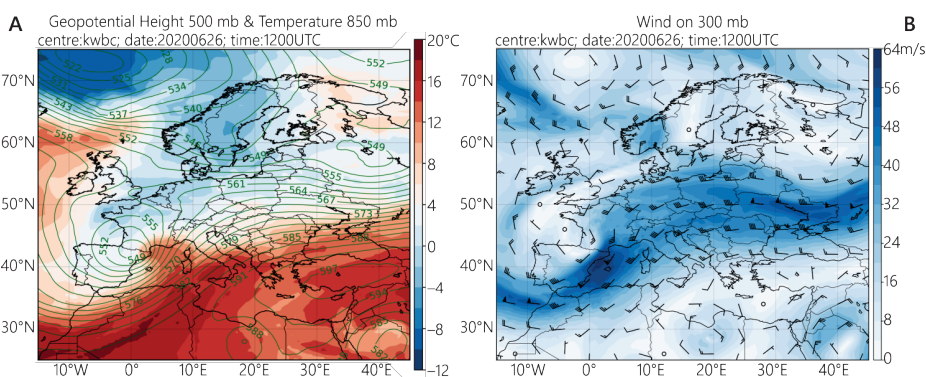


Figure 6. The same as Figure 4, but for 26.06.2020 in 12 UTC.

A comparison of Figures 5 and 6 suggests that it is not important whether the jet stream is north or south of Montenegro, but its position in relation to the jet stream's trough and ridge is important. In Figure 5, the trough of the jet stream is located just west of

Montenegro, which is associated with low pressure over Montenegro and locally strong winds, while in Figure 6, a jet stream ridge is located directly west of Montenegro, which is associated with high pressure over Montenegro, with light winds and mostly clear skies.

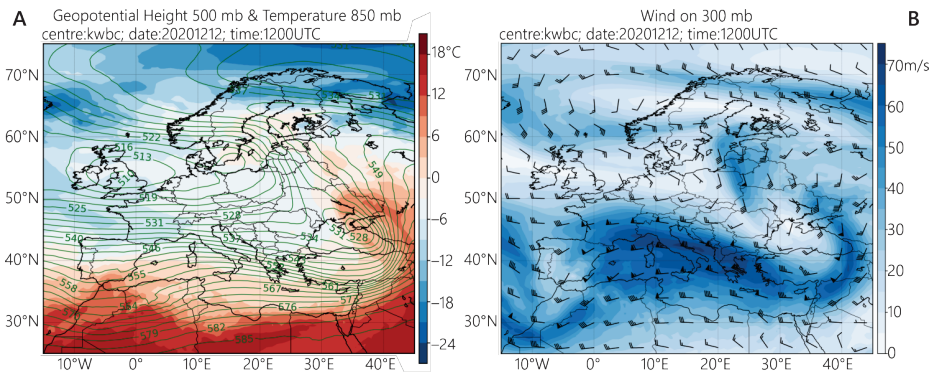


Figure 7. The same as Figure 4, but for 12.12.2020 in 12 UTC.

A typical saddle weather situation at the 500 hPa level on December 12, 2020 is shown in Figure 7: two centers of low pressure, over Great Britain and the Black Sea, and two areas of high pressure, over North Africa and northern Scandinavia. The saddle has formed between these pressure patterns, as a region of nearly stationary air. What the weather will be like in the saddle depends on the characteristics of the surface. Winter is imminent here, so cold air masses with light winds on the surface will lie over Central Europe and the Balkan Peninsula. The wind speed at the Krnovo wind farm site remained below 3 m/s on this day for 20 hours (or 120 10-minute intervals). During this time, there was a strong zonal flow at high altitudes, but the jet stream was intermittent over the Ukraine (Figure 7B). Despite the strong pressure gradient in the middle of the atmosphere (500 hPa), the wind over Montenegro is weak because a jet stream ridge was located immediately west of Montenegro, which is associated with a high pressure and light winds on the surface.

3.3. Verification of wind forecasts with the WRF NMM

The WRF NMM wind forecast was compared with the observed winds at a height of 90 m. The model error (ME, MA and RMSE) was larger in the early morning hours, which were characterized by the lowest mean wind speeds (see Appendix A, Figure A1). The numbers 24, 48, and 72 next to the error marks indicate the time interval of the forecast in hours. The magnitude of ME was highest at midnight and early in the morning, indicating that the model underestimated wind speeds more when they were weaker. MA24 was between 1.77 and 2.12 m/s, with the highest value measured in the early morning hours. It had the lowest values compared to MA48 and MA72. The RMSE24 were in an interval of 2.21 to 2.72 m/s. Two peaks occurred: a larger one in the early morning and a smaller one in the afternoon. This indicates a major modeling error in situations where abrupt changes in wind speeds occur at shorter time intervals. The analysis shows that the WRF-NMM model has a lower error in predicting higher wind speeds, which is confirmed by the minimum RMSE in the midday hours. This means that the prediction error is lower at higher and longer-lasting wind speeds. Therefore, the model is more accurate when forecasting higher wind speeds.

The model underestimated wind speeds throughout the year, except in May, September, and December. The RMSE showed the smallest error in spring and summer and the largest in winter. The extent of the error depends on the specific synoptic situations during the year. In October, March, and April, the efficiency of energy production was particularly high. This was due to the long periods with wind speeds of 14–25 m/s which occurred during these months. The model used to predict these wind speeds was very efficient, with relatively low RMSE values. This efficiency is particularly useful for estimating the MxEP.

The correlation coefficients (CC) for the hourly wind speed values were high for all forecast periods. For forecast periods of one, two, and three days, the coefficients were 0.85, 0.83, and 0.82, respectively (Figure 8). These values show that the WRF NMM is very efficient in predicting wind speeds up to three days in advance for the Krnovo wind farm site. These values were slightly higher than the correlation coefficient of the wind forecast of the Eta model at a similar height (98 m), which was 0.81 (Lazić et al., 2010). Figure 8 shows an underestimation of the wind speeds between 3–6 m/s, while the wind speeds in the range of 4–25 m/s show a strong correlation with the predicted values.

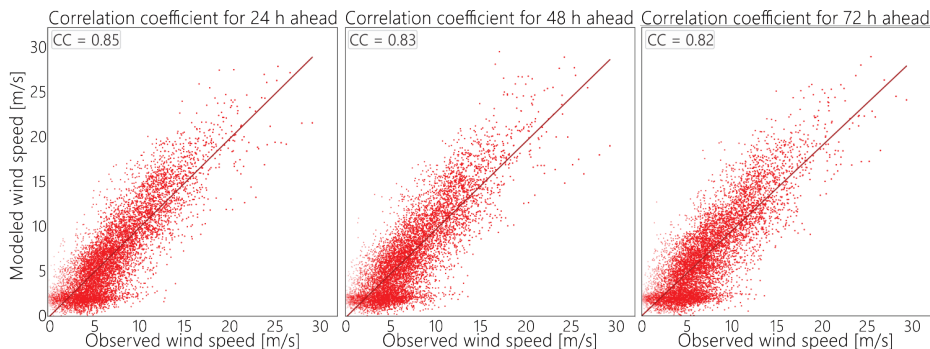


Figure 8. Correlation coefficient (CC) for forecasting periods of 24, 48 and 72 hours.

Table 2 shows the summarized results of the scalar measures for the accuracy of the wind forecast. Negative and relatively small ME values indicate that the model slightly underestimated the average hourly wind speeds. The smallest underestimation was for the 24-hour forecast period.

Table 2. Summary results of the verification parameters in comparing the WRF NMM forecast valid for 24, 48, and 72 hours against wind speed measurements.

ME24	ME48	ME72	MA24	MA48	MA72	RMSE24	RMSE48	RMSE72
-0.28	-0.33	-0.35	1.95	2.05	2.07	2.49	2.63	2.63

4. Conclusion

Two important contributions of this work are the verification of wind forecast over complex topography and the determination of a suitable synoptic situation for the maximum and minimum production of wind energy at the given location. A statistical analysis of the winds recorded in Krnovo (Nikšić) at a height of 90 m during the years 2019 and 2020 indicated that northerly and southerly winds were the most frequent in the area. They were present for most of the year (almost 65% of the year) and were the strongest. Wind speeds of 5 m/s were the

most frequent. More than 84% of the year, the wind speeds were higher than 3 m/s, so the wind turbines were in operation for over 7,380 hours per year. The wind was the strongest during the winter season, resulting in the highest electricity generation. The occurrence of the cut-out speed was rare and limited to two wind directions: North-East and South-South-East. This was due to occasional and isolated extreme weather conditions. These speeds were most likely caused by blizzards since they were recorded during the winter season.

The characteristic synoptic situations that lead to MxEP and MnEP over the complex terrain in the mountainous part of Montenegro have been identified. The most favorable weather situations for the MxEP were characterized by the existence of a deep trough at high altitudes over Western Europe, propagating in a northwest-southeast direction, together with a strongly pronounced meandering jet stream. Another favorable, but less frequent, synoptic situation was the occurrence of a strong cyclone over the UK. A particular weather pattern most typical of the MnEP is associated with a ridge or anticyclone over the Balkan Peninsula, a zonal jet stream on the 300 hPa surface and warm air advection over Montenegro at higher altitudes. The identification of synoptic situations characteristic of the MxEP and MnEP could improve the projection of power generation.

The WRF NMM model tended to underestimate the wind speeds at 90 m, especially when the speeds were low. However, the model performed better when predicting higher wind speeds, which are important for power generation. The accuracy of the wind forecast varies depending on the time of year. The prediction errors are greatest in winter, while they are comparatively smaller in spring and summer. However, the errors are not too significant and the correlation coefficients for all the three forecast periods are high. For lead times of one, two and three days, the correlation coefficients are 0.85, 0.83, and 0.82 respectively.

The results obtained from the early detection of the characteristic weather patterns for minimum and maximum energy production, together with reliable wind forecasts, are a very important contribution to the wind energy sector. They can help to improve the utilization of renewable energy in the future and make it more efficient. If the decision-makers at the wind farm know the synoptic situation a few days in advance, they can create a more efficient energy utilization system. The construction of further wind farms is planned in the wider vicinity of the investigated site, so the results of this study could be useful.

This is the first research of its kind in our region. However, the study has its limitations. Firstly, the analysis was carried out based on wind measurements from only two years. Secondly, due to the limited computer resources for generating, storing, and processing meteorological data, the model verification was only carried out for one year. For the same reason, the hodographs and thermodynamic diagrams could not be produced. However, the objective of the work was achieved, and typical synoptic situations leading to maximum or minimum energy production were identified. In future work, when much more data is available, a more comprehensive analysis should be carried out.

Acknowledgements

The Serbian Ministry of Education, Science and Technological Development partly supported the study under Grant number 451-03-136/2025-03/200162, and the Science Fund of the Republic of Serbia 10.13039/501100016047, No. 7389, Project EXTREMES. We sincerely thank Mr. Mirko Vujović and the Acuoenergy Firm (<https://masdar.ae/en/renewables/our-projects/krnovo-wind-farm>) for providing the observed wind data. We also appreciate Mr. Angel Marčev for

assisting us with the GRIB data, and Mr. Dragomir Bulatović for his help with the figures. We are very grateful to the Institute of Hydrometeorology and Seismology in Montenegro for allowing us to use the result of the numerical simulations for the research. The anonymous reviewers of this article and the journal's editor significantly contributed to the paper's quality, and we thank them for selfless contribution.

References

- American Meteorological Society. (2018). *Glossary of Meteorology*. <https://www.ametsoc.org/index.cfm/ams/publications/glossary-of-meteorology/>
- Association for Wind Energy in Europe. (2025). *Wind power share in the country's electricity mix* [Dataset]. Retrieved February 5, 2025, from <https://windeurope.org/about-wind/daily-wind/top-countries>
- Bilal, M., Solbakken, K., & Birkelund, Y. (2016). Wind speed and direction predictions by WRF and WindSim coupling over Nygardsfjell. *Journal of Physics: Conference Series*, 753(8), Article 082018. <https://doi.org/10.1088/1742-6596/753/8/082018>
- Burić, M., Micev, B., & Mitrović, L. (2012). *Atlas klime Crne Gore* [Climate Atlas of Montenegro]. Montenegrin Academy of Sciences and Arts.
- Burlando, M., Podestà, A., Villa, L., Ratto, C. F., & Cassulo, G. (2009). Preliminary estimate of the large-scale wind energy resource with few measurements available: The case of Montenegro. *Journal of Wind Engineering and Industrial Aerodynamics*, 97(11–12), 497–511. <https://doi.org/10.1016/j.jweia.2009.07.011>
- Carta, J. A., Ramírez, P., & Velázquez, S. (2009). A review of wind speed probability distributions used in wind energy analysis case studies in the Canary Islands. *Renewable and Sustainable Energy Reviews*, 13(5), 933–955. <https://doi.org/10.1016/j.rser.2008.05.005>
- Cuevas-Figueroa, G., Stansby, P. K., & Stallard, T. (2022). Accuracy of WRF for prediction of operational wind farm data and assessment of influence of upwind farms on power production. *Energy*, 254(Part B), Article 124362. <https://doi.org/10.1016/j.energy.2022.124362>
- Đurišić, Ž., & Mikulović, J. (2012). Assessment of the wind energy resource in the South Banat region, Serbia. *Renewable and Sustainable Energy Reviews*, 16(5), 3014–3023. <https://doi.org/10.1016/j.rser.2012.02.026>
- Energy Information Administration. (2021). *Annual Energy Outlook 2021 with projections to 2050*. https://www.eia.gov/outlooks/aeo/pdf/AEO_Narrative_2021.pdf
- Fonseca, R., Temimi, M., Thota, M. S., Nelli, N. R., Weston, M. J., Suzuki, K., Uchida, J., Kumar, K. N., Branch, O., Wehbe, Y., Al Hosari, T., Al Shamsi, N., & Shalaby, A. (2020). On the analysis of the performance of WRF and NICAM in a hyperarid environment. *Weather Forecast*, 35(5), 891–919. <https://doi.org/10.1175/WAF-D-19-0210.1>
- Frank, A., Lenearts, T., Radusinović, S., Spalevic, V., & Nyssen, J. (2016). The regional geomorphology of Montenegro mapped using Land Surface Parameters. *Zeitschrift für Geomorphologie*, 60(1), 21–34. <https://doi.org/10.1127/zfg/2016/0221>
- Italian Ministry for the Environment, Land and Sea. (2007). *Assessment of the Projects Potential in the Fields of Renewable Energy Sources, Energy Efficiency and Forestry Management, in the Framework of Clean Development Mechanism of the Kyoto Protocol in the Republic of Montenegro*. https://www.mase.gov.it/sites/default/files/archivio/allegati/CDM/2007/montenegro_report_EN.PDF
- Janjić, Z. I. (1994). The Step-Mountain Eta Coordinate Model: Further Developments of the Convection, Viscous Sublayer, and Turbulence Closure Schemes. *Monthly Weather Review*, 122(5), 927–945. [https://doi.org/10.1175/1520-0493\(1994\)122%3C0927:TSMECM%3E2.0.CO;2](https://doi.org/10.1175/1520-0493(1994)122%3C0927:TSMECM%3E2.0.CO;2)
- Janjic, Z. I. (2003). A Non-Hydrostatic Model Based on a New Approach. *Meteorology and Atmospheric Physics*, 82, 271–285. <https://doi.org/10.1007/s00703-001-0587-6>
- Janjic, Z. I., Gerrity, J. P. Jr, Nickovic, S. (2001). An Alternate Approach to Non-Hydrostatic Modeling. *Monthly Weather Review*, 129, 1164–1178. [https://doi.org/10.1175/1520-0493\(2001\)129%3C1164:AAATNM%3E2.0.CO;2](https://doi.org/10.1175/1520-0493(2001)129%3C1164:AAATNM%3E2.0.CO;2)
- Jiménez, P. A., & Dudhia, J. (2013). On the Ability of the WRF Model to Reproduce the Surface Wind Direction over Complex Terrain. *Journal of Applied Meteorology and Climatology*, 52(7), 1610–1617. <https://doi.org/10.1175/JAMC-D-12-0266.1>

- Köhler, C., Steiner, A., Saint-Drenan, Y.-M., Ernst, D., Bergmann-Dick, A., Zirkelbach, M., Bouallègue, Z. B., Metzinger, I., & Ritter, B. (2017). Critical weather situations for renewable energies–Part B: Low stratus risk for solar power. *Renewable Energy*, 101, 794–803. <https://doi.org/10.1016/j.renene.2016.09.002>
- Krishnamurthy, V. (2019). Predictability of Weather and Climate. *Earth and Space Science*, 6(7), 1043–1056. <https://doi.org/10.1029/2019EA000586>
- Landberg, L. (2016). *Meteorology for Wind Energy: An Introduction*. John Wiley & Sons.
- Lazić, L., Pejanović, G., & Živković, M. (2010). Wind forecasts for wind power generation using the Eta model. *Renewable Energy*, 35(6), 1236–1243. <https://doi.org/10.1016/j.renene.2009.10.028>
- Lazić, L., Pejanović, G., & Živković, M. (2014). Improved wind forecasts for wind power generation using the Eta model and MOS (Model Output Statistics) method. *Energy*, 73, 567–574. <https://doi.org/10.1016/j.energy.2014.06.056>
- Lee, J. C. Y., Draxl, K. & Berg, L. K. (2022). Evaluating wind speed and power forecasts for wind energy applications using an open-source and systematic validation framework. *Renewable Energy*, 200, 457–475, <https://doi.org/10.1016/j.renene.2022.09.111>
- Masdar. (2025). *Krnovo Wind Farm*. <https://masdar.ae/en/renewables/our-projects/krnovo-wind-farm>
- Ministarstvo energetike i rudarstva. (2024). *Izveštaj o realizaciji energetskeg bilansa za 2023. godinu* [Report on the realisation of the energy balance for the year 2023]. <https://www.gov.me/dokumenta/1d6835df-d73b-49f9-988e-9947af258831>
- Potić, I., Joksimović, T., Milinčić, U., Kićović, D., & Milinčić, M. (2021). Wind energy potential for the electricity production–Knjaževac Municipality case study (Serbia). *Energy Strategy Reviews*, 33, Article 100589. <https://doi.org/10.1016/j.esr.2020.100589>
- Romanic, Dj., Parvu, D., Refan, M., & Hangan, H. (2018). Wind and tornado climatologies and wind resource modelling for a modern development situated in “Tornado Alley”. *Renewable Energy*, 115, 97–112. <https://doi.org/10.1016/j.renene.2017.08.026>
- Souza, N. B. P., Nascimento, E. G. S., & Moreira, D. M. (2023). Performance evaluation of the WRF model in a tropical region: Wind speed analysis at different sites. *Atmosfera*, 36(2), 253–277. <https://doi.org/10.20937/atm.52968>
- Steiner, A., Köhler, C., Metzinger, I., Braun, A., Zirkelbach, M., Ernst, D., Tran, P., & Ritter, B. (2017). Critical weather situations for renewable energies–Part A: Cyclone detection for wind power. *Renewable Energy*, 101, 41–50. <https://doi.org/10.1016/j.renene.2016.08.013>
- Tan, E., Sibel Mentess, S., Unal, E., Unal, Y., Efe, B., Barutcu, B., Onol, B., Sema Topcu, H., & Incecik, S. (2021). Short term wind energy resource prediction using WRF model for a location in western part of Turkey. *Journal of Renewable and Sustainable Energy*, 13, Article 013303. <https://doi.org/10.1063/5.0026391>
- Tong, W. (2010). Fundamentals of wind energy. In W. Tong (Ed.), *Wind Power Generation and Wind Turbine Design* (pp. 3–48). WIT Press.
- Valappil, V. K., Temimi, M., Weston, M., Fonseca, R., Nelly, N. R., Thota, M., & Kumar, K. N. (2020). Assessing Bias Correction Methods in Support of Operational Weather Forecast in Arid Environment. *Asia-Pacific Journal of Atmospheric Sciences*, 56, 333–347. <https://doi.org/10.1007/s13143-019-00139-4>
- Weibull, W. (1951). A Statistical Distribution Function of Wide Applicability. *Journal of Applied Mechanics*, 18(3), 293–297. <https://jhanley.biostat.mcgill.ca/bios601/CHchapters040506/Weibull-ASME-Paper-1951.pdf>
- Wilks, D. S. (2006). *Statistical Methods in the Atmospheric Sciences* (2nd ed.). Academic Press.
- Wood, N., & Mason, P. (1993). The pressure force induced by neutral, turbulent flow over hills. *Quarterly Journal of Royal Meteorological Society*, 119(514), 1233–1267. <https://doi.org/10.1002/qj.49711951402>
- Wyszogradzki, A. A., Liu, Y., Jacobs, N., Childs, P., Zhang, Y., Roux, G., & Warner, T. T. (2013). Analysis of the surface temperature and wind forecast errors of the NCAR-AirDat operational CONUS 4-km WRF forecasting system. *Meteorological and Atmospheric Physics*, 122, 125–143. <https://doi.org/10.1007/s00703-013-0281-5>
- Zečević, A., Filipović, L., & Marčev, A. (2023). Verification of temperature, wind and precipitation fields for the high-resolution WRF NMM model over the complex terrain of Montenegro. *Technology and Health Care*, 31(4), 1525–1539. <https://doi.org/10.3233/THC-229016>
- Zorić, M. (1976). Visoravan Krnovo u Crnoj Gori [Krnovo plateau in Montenegro]. *Priroda*, 65(7), 207–212. <https://library.foi.hr/dbook/cas.php?B=1&item=S00001&godina=1976&broj=00007&page=207>

Appendix A

Table A1. Summary results of the verification parameters and correlation coefficient in comparing the WRF NMM forecast against wind speed measurements

	Max	Mean	Min	Std	25%	50%	75%
January	24.58	7.80	0.25	4.23	4.61	7.16	10.35
February	31.51	9.22	0.35	5.23	4.85	8.30	13.04
March	23.50	7.55	0.32	3.74	4.90	7.07	9.73
April	24.72	7.05	0.43	3.67	4.38	6.60	8.83
May	20.39	6.86	0.22	3.47	4.24	6.54	8.84
June	20.47	5.30	0.00	3.17	3.02	4.79	7.01
July	16.39	5.51	0.00	3.08	3.24	5.17	7.31
August	17.42	4.85	0.00	2.67	2.90	4.57	6.45
September	25.28	5.78	0.00	3.53	3.34	5.23	7.65
October	23.48	5.86	0.00	3.51	3.37	5.16	7.66
November	22.90	7.25	0.00	4.47	4.17	6.25	9.85
December	29.53	8.41	0.00	4.88	4.74	7.50	11.9

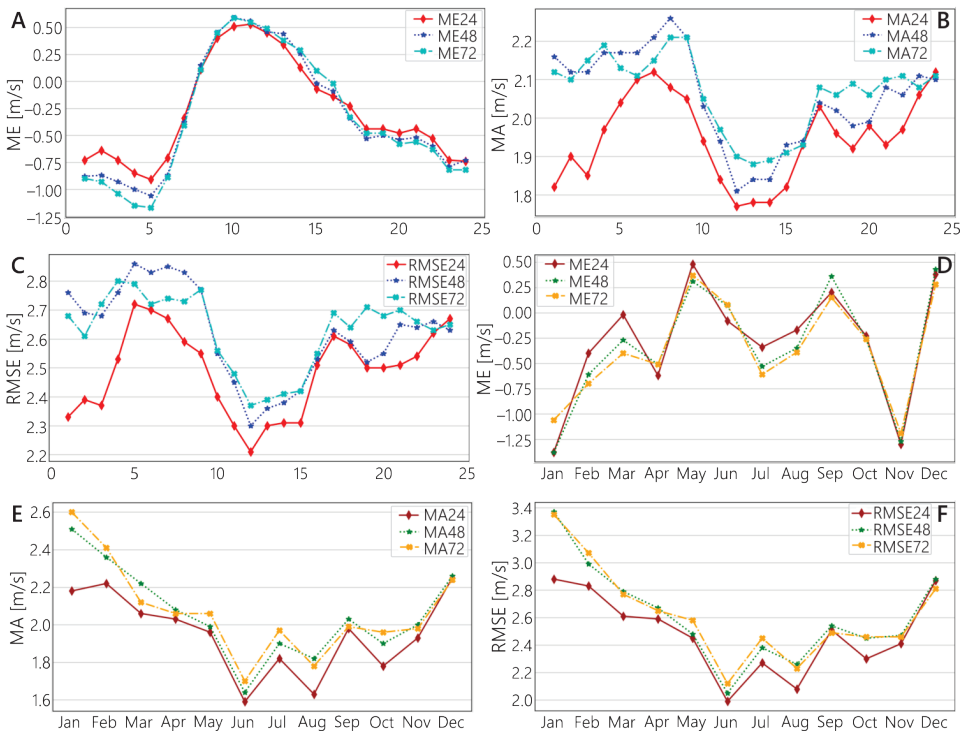


Figure A1. Hourly and monthly variations of the mean error (ME), the mean absolute error (MA) and the root mean square error (RMSE) of the NMM WRF model forecast compared to the wind observations.

